JOURNAL OF VIROLOGY, Jan. 2008, p. 300–310 Vol. 82, No. 1
0022-538X/08/$08.00+0 doi:10.1128/JVI.01794-07

Type I Interferons Are Essential in Controlling Neurotropic Coronavirus Infection Irrespective of Functional CD8 T Cells▽

Derek D. C. Ireland,[1] Stephen A. Stohlman,[1] David R. Hinton,[2] Roscoe Atkinson,[2] and Cornelia C. Bergmann[1]*

Department of Neuroscience, Lerner Research Institute, The Cleveland Clinic, Cleveland, Ohio 44195,[1] and Department of Pathology, University of Southern California Keck School of Medicine, Los Angeles, California 90033[2]

Received 15 August 2007/Accepted 28 September 2007

Neurotropic coronavirus infection induces expression of both beta interferon (IFN-β) RNA and protein in the infected rodent central nervous system (CNS). However, the relative contributions of type I IFN (IFN-I) to direct, cell-type-specific virus control or CD8 T-cell-mediated effectors in the CNS are unclear. IFN-I receptor-deficient (IFNAR$^{-/-}$) mice infected with a sublethal and demyelinating neurotropic virus variant and those infected with a nonpathogenic neurotropic virus variant both succumbed to infection within 9 days. Compared to wild-type (wt) mice, replication was prominently increased in all glial cell types and spread to neurons, demonstrating expanded cell tropism. Furthermore, increased pathogenesis was associated with significantly enhanced accumulation of neutrophils, tumor necrosis factor alpha, interleukin-6, chemokine (C-C motif) ligand 2, and IFN-γ within the CNS. The absence of IFN-I signaling did not impair induction or recruitment of virus-specific CD8 T cells, the primary adaptive mediators of virus clearance in wt mice. Despite similar IFN-γ-mediated major histocompatibility complex class II upregulation on microglia in infected IFNAR$^{-/-}$ mice, class I expression was reduced compared to that on microglia in wt mice, suggesting a synergistic role of IFN-I and IFN-γ in optimizing class I antigen presentation. These data demonstrate a critical direct antiviral role of IFN-I in controlling virus dissemination within the CNS, even in the presence of potent cellular immune responses. By limiting early viral replication and tropism, IFN-I controls the balance of viral replication and immune control in favor of CD8 T-cell-mediated protective functions.

Interferons (IFN), originally named for interfering with virus replication, comprise a pleiotropic family of cytokines that participate in many aspects of innate and adaptive immunity. Induction of type I IFN (IFN-I), including alpha IFN (IFN-α) and IFN-β, is triggered by a variety of cellular pattern recognition receptors in response to various pathogen-specific structures, including double-stranded RNA, single-stranded RNA, and viral RNA with unprotected 5′-triphosphates (21, 46). Release of IFN-I and subsequent signaling in the same cell or neighboring cells amplify the original signal by triggering transcription of numerous IFN-α family members and IFN-inducible genes, thus inducing an antiviral state. Pathways of IFN-I induction, signal transduction, and antiviral mechanisms have been well characterized (21, 46). The cellular ability to sense viral nucleic acids via cytosol-localized helicase receptors or endosomal localized toll-like receptors (TLR) allows IFN-I activation not only in infected cells but also in cells that have acquired viral RNA in endosomes. As expression of TLR family members is restricted in many cell types, the mechanisms underlying initiation of IFN-I induction are thus not only virus, but also cell type, specific and thus dependent on in vivo tropism and tissue milieu (46, 57). Specialized plasmacytoid dendritic cells (pDC) in lymphoid tissue produce especially high levels of IFN-I upon some viral infections (21).

IFN-I can thus exert antiviral effects at multiple levels including induction of antiviral genes, augmentation of antigen-presenting cell function, and regulation of lymphocyte function and survival (46). For example, IFN-I have been proposed as a third signal required for full CD8 T-cell activation (10) and as a survival signal for CD8 T cells in response to lymphocytic choriomeningitis virus (LCMV) infection (22). However, the IFN-I requirement for T cells for survival is determined by the innate microenvironment generated in response to a particular pathogen. During LCMV infection, which elicits high IFN-I levels, virus-specific T cells are exquisitely dependent on IFN-I for survival. By contrast, during virus infections eliciting lower IFN-I levels, T cells are less dependent on IFN-I (48).

Direct antiviral functions are especially critical to preserve terminally differentiated cells and limit viral spread during central nervous system (CNS) infections, prior to induction and recruitment of adaptive immune effectors. The CNS is unique in many immunological aspects, including the absence of conventional lymphatic drainage and pDC or other DC in the parenchyma, the paucity of major histocompatibility complex (MHC) expression on resident cells, and restricted leukocyte entry due to the blood-brain barrier anatomy (16, 42). Constitutive production of IFN-α by neurons and glial cells has been linked to several homeostatic processes (11). Viral infections can also upregulate IFN-I production by neurons and glial cells (12, 38). In addition to the capacities of inducing an antiviral state, IFN-I also drives expression of a variety of immunomodulatory genes including cytokine, chemokine, adhesion molecule, MHC, and costimulatory molecule genes in different CNS-resident cells (2, 12, 38). Protection afforded by IFN-I is clearly demonstrated by uncontrolled replication during CNS infection with Sindbis virus, West Nile virus, and

* Corresponding author. Mailing address: The Cleveland Clinic, 2500 Euclid Avenue, NC30, Cleveland, OH 44195. Phone: (216) 444-5922. Fax: (216) 444-7927. E-mail: bergmac@ccf.org.

▽ Published ahead of print on 10 October 2007.

vesicular stomatitis virus (31, 40, 41). The cellular sources of IFN-I during CNS infections have not been extensively studied. Rabies virus induces the production of IFN-I by TLR-3-expressing neurons in vitro (36). West Nile virus drives the production of IFN-I in the CNS to protect neurons from infection and death (41). In the case of Sindbis virus infection, the outcome is dependent on the viral strain analyzed, with more-virulent strains being lethal in IFN-deficient mice and less-virulent strains producing almost no disease (40). Together, these findings suggest that the role of IFN-I during infection is virus dependent.

The roles of IFN-I in controlling neurotropic coronavirus (CoV) infections are poorly defined. Several members of the *Coronaviridae* family, including the severe acute respiratory syndrome-CoV and mouse hepatitis virus (MHV), have recently been shown to avoid recognition by cytoplasmic pattern recognition receptors (51, 57). These studies confirmed earlier findings demonstrating that MHVs are poor IFN-β inducers in fibroblast cells (17, 52, 56). Importantly, the absence of IFN-I induction in fibroblasts could not be attributed to the absence of double-stranded RNA during viral replication or inhibition of IFN-β signaling (51, 56), unlike IFN antagonists uncovered in severe acute respiratory syndrome-CoV (23, 45). Nevertheless, a recent study proposes that MHV-A59 nucleocapsid protein may act as an IFN-I antagonist (55). In contrast to the inability of MHV to trigger IFN-I in fibroblasts, peripheral infection by the liver- and CNS-tropic MHV-A59 strain induces IFN-I expression, primarily initiated by pDC in a TLR-7-dependent mechanism (8). Furthermore, MHV infections of primary neuronal cultures as well as the CNS also induce IFN-β mRNA (37, 39, 58), demonstrating that MHV-mediated IFN-I induction is not restricted to pDC in vivo. Gene profiling of neuronal cultures infected with the neurotropic MHV-JHM further revealed upregulation of IFN-I-induced transcription factors, as well as induction of MHC class I heavy chains, nonclassical class I molecules, and multiple cofactors involved in class I antigen processing (38). An in vivo role for IFN-I is supported by MHC class I upregulation in microglia following sublethal MHV-JHM infection of IFN-γ-deficient mice (5). These results, in addition to CoV sensitivity to IFN-I in vitro (17), exacerbated disease in the presence of anti-IFN antibodies (24), and increased resistance to MHV virulence caused by IFN-β treatment in vivo (29, 44), all implicate IFN-I as a crucial player in host defense against CNS CoV infection. Furthermore, peripheral infection of mice deficient in a functional receptor, IFN-I receptor (IFNAR$^{-/-}$), with MHV-A59 resulted in increased viral replication and systemic spread, including the CNS (8).

This study further explores the role of IFN-I in innate and adaptive antiviral functions in a model of sublethal MHV-induced encephalitis associated with demyelination. The sublethal, glia-tropic MHV-JHM variant v2.2-1 replicates exclusively in the CNS following intracranial infection and is primarily controlled by CD8 T cells (4). The complex interplay of cell-type-specific induction of IFN-I by MHV, its sensitivity to direct antiviral IFN-I activity, and potential CD8 T-cell dependence on IFN-I prompted an investigation into the direct antiviral effects versus CD8 T-cell-mediated protection using IFNAR$^{-/-}$ mice. The data clearly demonstrate that IFN-I-dependent innate responses are essential in controlling CNS replication and host survival. CD8 T-cell expansion, recruitment, and function were not impaired, suggesting that adaptive responses are insufficient in controlling viral CNS spread, once the virus expands its tropism and replication exceeds a certain threshold.

MATERIALS AND METHODS

Animals and viruses. C57BL/6 mice were purchased from the National Cancer Institute (NCI, Frederick, MD). C57BL/6-IFNAR$^{-/-}$ mice were kindly provided by Kaja Murali-Krishna (22) (University of Washington, Seattle, WA) and bred under pathogen-free conditions. Mice were housed at either the University of Southern California animal facility or the Biological Resources Unit of the Cleveland Clinic. All procedures were performed in compliance with protocols approved by the Institutional Animal Care and Use Committees of the Keck School of Medicine and the Cleveland Clinic.

Mice were infected at 6 weeks of age by intracranial injection with 250 PFU of the glia-tropic MHV-JHM variant V2.2-1 in 30 μl endotoxin-free Dulbecco's phosphate-buffered saline (DPBS) (13). In some experiments mice were infected with a dual monoclonal antibody (MAb)-derived variant of MHV-JHM designated V2.2/7.2-2. This neurotropic variant replicates to levels within the CNS similar to those of V2.2-1 but does not induce clinical disease or myelin loss (14, 26). Neutrophils were depleted by intraperitoneal administration of 200 μg anti-Ly-6G/C (RB6-8C5) MAb at days −1, +1, +3, and +5 postinfection (p.i.). Control mice received 200 μg MAb GL113, specific for β-galactosidase. Following intraperitoneal administration of ketamine-xylazine (100 and 10 mg/kg of body weight, respectively), blood was collected from infected mice by cardiac puncture and mice were perfused intracardially with 10 ml DPBS. Brain, serum, cervical lymph nodes (CLN), and spleen were collected for analysis.

CNS virus and isolation of inflammatory cells. Brains were bisected sagittally. One half-brain from each mouse was homogenized in ice-cold Ten Broeck glass grinders in 4 ml of DPBS. Homogenates were clarified by centrifugation for 7 min at 400 × *g*. Supernatants were stored at −80°C. MHV-JHM in supernatants was measured by plaque assay on monolayers of delayed brain tumor astrocytoma cells as previously described (13). Inflammatory cells were recovered from the pellets as previous described (3). Briefly, cell pellets were resuspended in RPMI supplemented with 1% fetal calf serum and 25 mM HEPES (supplemented RPMI) and adjusted to 30% Percoll (Pharmacia, Uppsala, Sweden). Following addition of a 1-ml 70% Percoll underlay, cells were collected at the 30%-70% Percoll interface after centrifugation at 800 × *g* for 30 min, washed in supplemented RPMI, and resuspended in 1 ml supplemented RPMI. Cells from the spleen and CLN were isolated by disrupting tissue in 5 ml of supplemented RPMI. Splenocytes were treated with Gey's solution to lyse erythrocytes, washed, and resuspended in 5 ml supplemented RPMI.

Flow cytometry. Cell surface staining for four-color flow cytometry was used to analyze cell populations isolated from the brain, spleen, and CLN. Cells were incubated with 1% polyclonal mouse serum and 1% rat anti-mouse FcγIII/IIR MAb in fluorescent antibody cell sorting (FACS) buffer (0.5% bovine serum albumin in DPBS) for 20 min at 4°C to block nonspecific binding. Specific cell types were identified using a fluorescein isothiocyanate-, phycoerythrin-, peridinin chlorophyll protein (PerCP)-, or allophycocyanin-conjugated anti-mouse MAb: CD4 (GK1.5), CD8 (53.67), Ly-6G (1G9), I-A/I-E (M5/114.15.2), and H2-D^b (KH95) (all from BD Biosciences, San Diego, CA) and F4/80 (CI:A3-1; Serotec, Raleigh, NC). Virus-specific CD8 T cells were identified using H-2D^b/S510 MHC class I tetramers as described previously (3). Cells were incubated with antibodies for 30 min on ice, washed twice with FACS buffer, and fixed with 2% paraformaldehyde for 10 min on ice. Intracellular staining for IFN-γ was performed as described previously (60). Briefly, 1×10^6 brain cells were incubated for 6 h at 37°C with 1×10^5 EL-4 (H-2D^b) or CHB3 (I-A^b) stimulator cells (18) in 200 μl of RPMI containing 10% FCS and 1 μl/ml Golgi-stop (BD Biosciences) in the presence or absence of peptide. S510 peptide (spike protein amino acids 510 to 518) comprising the immunodominant D^b CD8 T-cell epitope was used at 1 μM (EL-4 cells), and M133 peptide (matrix protein amino acids 138 to 147) comprising the I-A^b CD4 T-cell epitope (CHB3 cells) was used at 5 μM. Cells were stained with PerCP-conjugated anti-CD8 (53.67) MAb, fixed and permeabilized with Cytofix/Cytoperm (BD Biosciences), and subsequently stained with fluorescein isothiocyanate-conjugated anti-IFN-γ MAb (XMG1.2) (BD Biosciences). At least 100,000 events were acquired on a FACSCalibur flow cytometer (BD Biosciences) for subsequent data analysis using Flow-Jo 7 software (Tree Star, Inc., Ashland, OR).

Cytokine determination. Cytokines in brain homogenate supernatants were measured by cytometric bead array (CBA) using the mouse inflammation CBA

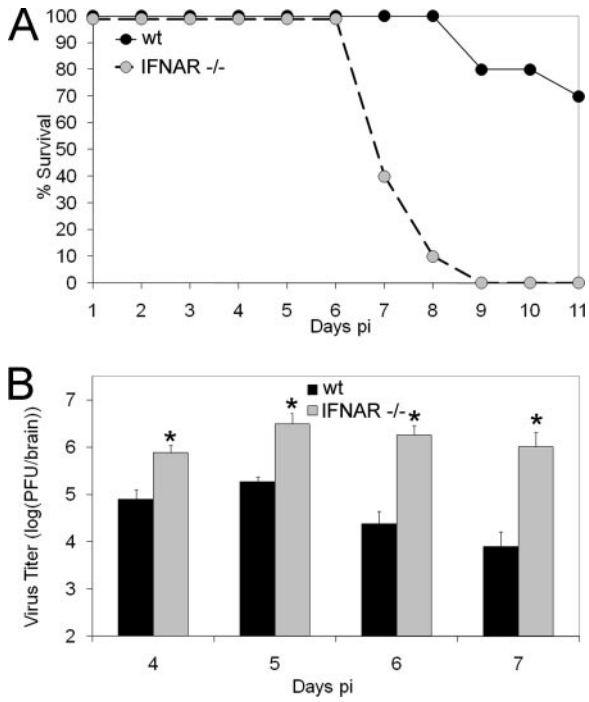

FIG. 1. IFN-I signaling is required for protection from glia-tropic MHV-JHM infection. (A) Survival rates of wt and IFNAR$^{-/-}$ mice (n = 15/group) after infection with MHV-JHM. (B) Virus replication (PFU/brain) in the brain following infection. Data are the means of three to six mice per time point ± standard errors of the means. Asterisks indicate statistical significance ($P \leq 0.05$) in comparison to wt mice.

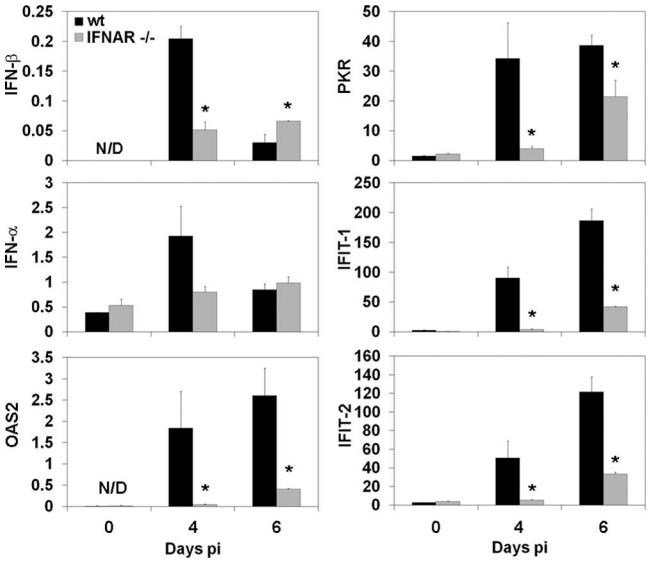

FIG. 2. CNS expression of IFN-I and IFN-stimulated genes in response to infection. Brains from uninfected (0) and infected (day 4 and 6) wt and IFNAR$^{-/-}$ mice were analyzed for mRNA levels of IFN-β, IFN-α, and IFN-stimulated gene products OAS2, PKR, IFIT-1, and IFIT-2 by quantitative real-time PCR (n = 3 mice per time point). Data are calculated as levels relative to the housekeeping gene product glyceraldehyde-3-phosphate dehydrogenase and representative of two independent experiments. N/D, not detected. Asterisks indicate statistical significance ($P \leq 0.05$) in comparison to wt mice.

kit according to the manufacturer's protocol (BD Biosciences). Briefly, 50 μl of homogenate, undiluted or diluted 10-fold, was mixed with 50 μl of beads and 50 μl of phycoerythrin detection buffer and then incubated for 2 h at room temperature. Beads were washed, and acquisition was performed using a FACSCalibur (BD Biosciences) flow cytometer. Data analysis was performed using the CBA analytical software (BD Biosciences).

Histopathological analysis. One half-brain and spinal cords from each mouse were fixed with Clark's solution (75% ethanol and 25% glacial acetic acid) and embedded in paraffin. Sections were stained with either hematoxylin and eosin or Luxol Fast Blue as described previously (5). Distribution of viral antigen was determined by immunoperoxidase staining (Vectastain-ABC kit; Vector Laboratories, Burlingame, CA) using the anti-MHV-JHM MAb J.3.3 specific for the carboxyl terminus of the viral nucleocapsid protein as primary antibody, horse anti-mouse antibody as secondary antibody, and 3,3′-diaminobenzidine substrate (Vector Laboratories) (5). Sections were scored for inflammation and viral antigen in a blinded fashion. Representative fields were identified based on average scores of all sections in each experimental group.

Real-time PCR. Half-brains were immediately placed into 1 ml TRIzol (Invitrogen, Carlsbad, CA) and homogenized in sterile Ten Broeck glass grinders. RNA was purified according to the manufacturer's protocol (Invitrogen, CA). Briefly, 0.2 ml chloroform (Sigma-Aldrich, St. Louis, MO) was added to 1 ml of homogenate, mixed, and centrifuged at 12,000 × g for 15 min at 4°C. RNA was precipitated from the aqueous phase by addition of 0.5 ml isopropyl alcohol and centrifugation at 12,000 × g for 10 min at 4°C, washed in 75% ethanol, and resuspended in diethyl pyrocarbonate-treated H_2O. The concentration and purity of RNA were measured by spectrophotometry at 260/280 nm. RNA integrity was confirmed by electrophoresis on 1.2% formaldehyde gels.

DNA contamination was eliminated by treatment with DNase I (Roche, Palo Alto, CA) for 30 min at 37°C in the presence of RNasin (Promega, Madison, WI). DNase I was heat inactivated in the presence of 10 mM EDTA at 70°C for 5 min. Reverse transcription was performed on 2 μg RNA, primed with 1 μg random hexamers (Promega) using avian myeloblastosis virus reverse transcriptase (Promega) for 1 h at 42°C. Real-time PCR was performed using CYBR Green Master Mix (Applied Biosystems, Foster City, CA). Real-time primer sequences were as follows: IFIT-1 (ISG-56), F, 5′-CCTTTACAGCAACCATG GGAGA-3′, and R, 5′-GCAGCTTCCATGTGAAGTGAC-3′; IFIT-2 (ISG-54), F, 5′-AGAGGAAGAGGTTGCCTGGA-3′, and R, 5′-CTCGTTGTACTCATG ACTGCTG-3′; 2′-5′ oligoadenylsynthetase (OAS2), F, 5′-AAAAATGTCTGC TTCTTGAATTCTGA-3′, and R, 5′-TGTGCCTTTGGCAGTGGAT-3′; protein kinase R (PKR), F, 5′-GGCTCCTGTGTGGGAAGTCA-3′, and R, 5′-TA TGCCAAAAGCCAGAGTCCTT-3′; IFN-α, F, 5′-CCTGAGAGAGAAGAAA CACAGC-3′, and R, 5′-GAGGAAGACAGGGCTCTCC-3′; IFN-β, F, 5′-GC TCCTGGAGCAGCTGAATG-3′, and R, 5′-CGTCATCTCCATAGGGATCT TGA-3′. Real-time PCR was performed using an MJ Research Opticon DNA engine, with Opticon Monitor software (Bio-Rad, Hercules, CA) under the following conditions: 95°C for 10 min and 40 cycles of denaturation at 94°C for 10 s, elongation at 60°C for 20 s, and annealing at 76°C for 1 s. All data presented are expressed as induction (n-fold) based on the following formula: $(2^{[CT\{\text{GAPDH}\} - CT\{\text{target}\}]}) \times 1{,}000$, where C_T is threshold cycle and GAPDH is glyceraldehyde-3-phosphate dehydrogenase.

Statistical analysis. Student's t test with equal variance was used to compare IFNAR$^{-/-}$ and wild-type (wt) mice. Significant differences between groups are noted with an asterisk in the figures ($P \leq 0.05$).

RESULTS

IFN-I signaling is essential for control of glia-tropic MHV-JHM infection in the CNS. MHV-mediated induction of IFN-β in the CNS (37, 39), as well as limited protection following peripheral and intranasal IFN-I treatment during MHV infection (29, 44), suggested a protective role against CoV infections. To directly assess the role of IFN-I in the CNS during glia-tropic CoV infections, MHV-JHM V2.2-1 pathogenesis was compared in IFNAR$^{-/-}$ and wt mice. Symptoms of encephalitis, including lethargy, hunched posture, and weight loss, developed more rapidly and were more severe in IFNAR$^{-/-}$ mice. All IFNAR$^{-/-}$ mice succumbed to infection by day 9 p.i., whereas mortality never exceeded 20% in wt mice

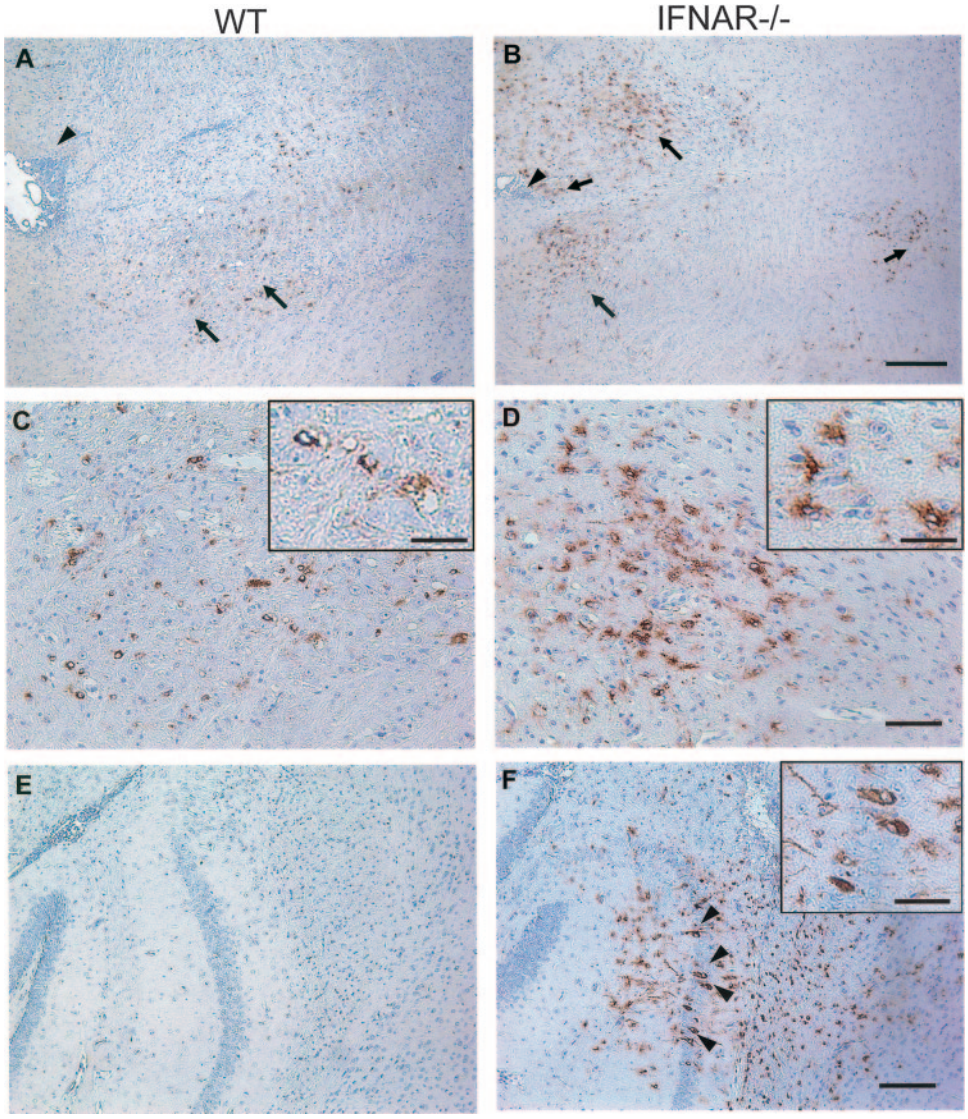

FIG. 3. Influence of IFN-I signaling on viral antigen distribution. Viral antigen detected by immunoperoxidase staining using MAb J.3.3 (red chromogen; hematoxylin counterstain) in brains from infected wt (A, C, and E) and IFNAR$^{-/-}$ (B, D, and F) mice at day 6 p.i. Arrows mark antigen-positive cells, and arrowheads mark perivascular inflammatory infiltrates (A and B). Note increased foci of viral antigen-positive cells in deep cerebral white matter (B and D) and in glial cells and hippocampus pyramidal neurons (arrowheads) (F) in the absence of IFN-α/β signaling. Bars, 200 μm (A and B), 50 μm (25 μm for inset) (C and D), and 100 μm (40 μm for inset) (E and F).

(Fig. 1A). Infectious virus in the CNS was examined to ensure that increased mortality correlated with increased virus replication. Higher levels of virus were present in the CNS of IFNAR$^{-/-}$ mice at days 4 and 5 p.i. compared to wt mice, suggesting that IFN-I contributes to early control of virus replication (Fig. 1B). Virus in the CNS of wt mice peaked at day 5 p.i and then declined, consistent with T-cell-mediated clearance (5). By contrast, virus titers in the CNS of IFNAR$^{-/-}$ mice were not significantly reduced by day 7 p.i. Little or no apparent control of infectious virus in IFNAR$^{-/-}$ mice suggested that increased mortality was associated with uncontrolled virus replication. To test whether IFN-I signaling was equally essential in controlling a nonpathogenic MHV-JHM variant, IFNAR$^{-/-}$ mice were infected with the neurotropic V2.2/7.2-2 variant (14). This variant is controlled in wt mice without evidence of clinical symptoms or demyelination (14, 26). IFNAR$^{-/-}$ mice also rapidly succumbed to this infection, which was accompanied by uncontrolled virus replication (data not shown). These results demonstrate a requirement for IFN-I-dependent mechanisms to protect mice from fatal CoV-induced encephalitis.

CNS infection induces IFN-I and IFN response genes. To confirm that increased virus in the CNS of IFNAR$^{-/-}$ mice correlated with IFN-I signaling defects, mRNAs encoding IFN-β or IFN-α, as well as IFN-α/β response genes in the CNS, were analyzed in uninfected mice and at days 4 and 6 p.i. (Fig. 2). IFN-α and IFN-β mRNA were modestly induced in the CNS of both groups at day 4 p.i. The mRNAs encoding IFN-α and IFN-β declined by day 6 p.i. in wt mice. By contrast, the minimal induction of IFN-α and IFN-β mRNA in the CNS

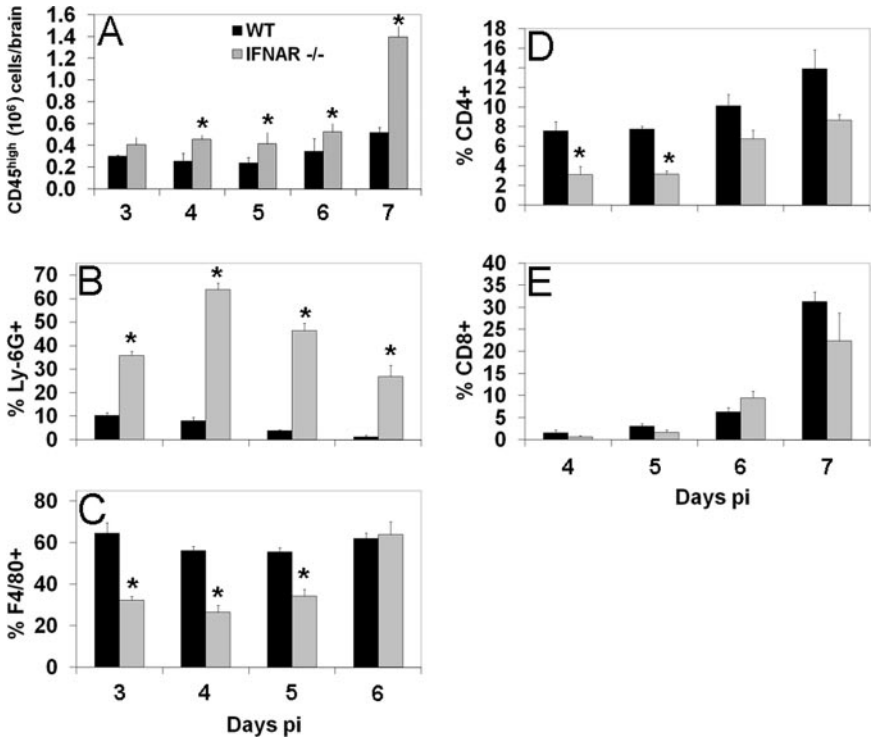

FIG. 4. Neutrophils dominate cell infiltrates in the CNS of IFNAR$^{-/-}$ mice. Numbers and composition of brain-infiltrating cells in infected wt and IFNAR$^{-/-}$ mice analyzed by flow cytometry at the indicated times p.i. (A) Numbers of bone marrow-derived CD45^{high} cells/brain. (B to E) Percentages of cell subsets within the infiltrating population identified as neutrophils (B), macrophages (C), CD4 T cells (D), and CD8 T cells (E). Data are the means of three experiments (pooled from three mice/group) per time point ± standard errors of the means. Asterisks indicate statistical significance ($P \leq 0.05$) in comparison to wt mice.

of infected IFNAR$^{-/-}$ mice remained constant between days 4 and 6 p.i. IFN-stimulated genes, including the antiviral OAS2, PKR, and IFN-induced protein with tetratricopeptide repeats 1 (IFIT-1) and IFIT-2 genes, were induced in the CNS of wt mice following infection. In comparison to wt mice, expression of these genes was reduced in the CNS of IFNAR$^{-/-}$ mice. Transcription of IFIT-1, IFIT-2, and especially PKR was upregulated in the CNS of both groups at day 6 p.i., although expression levels in IFNAR$^{-/-}$ mice were significantly reduced compared to infected wt mice. These data demonstrated induction of classical antiviral PKR- and OAS-mediated pathways and reduced transcription of these genes in IFNAR$^{-/-}$ mice prior to detection of IFN-γ (see below).

Impaired IFN-I signaling increases viral spread and tropism within the CNS. MHV-JHM initially infects ependymal cells and subsequently spreads to astrocytes and microglia/macrophages and finally to oligodendrocytes but rarely infects neurons (53). To determine if IFN-I preferentially protects a specific cell type, brain and spinal cord were analyzed for distribution of viral nucleocapsid antigen. Increased viral antigen, which appeared to include infected astrocytes, macrophages/microglia, and oligodendroglia, was detected in brains of infected IFNAR$^{-/-}$ mice compared to wt mice at all times analyzed (Fig. 3A and B). No preferential susceptibility of distinct glial subsets was noted in infected IFNAR$^{-/-}$ mice. However, in contrast to wt mice, in which only relatively isolated virus-infected cells were detected throughout the parenchyma (Fig. 3A and C), local foci of infected cells were prominent in the CNS of IFNAR$^{-/-}$ mice (Fig. 3B and D), suggesting rapid localized virus spread to adjacent cells. Although no virally infected cells were detected in the spinal cords derived from wt mice, a small number of cells were infected in the spinal cords of IFNAR$^{-/-}$ mice, consistent with increased infectious virus and infected cells in the brains of IFNAR$^{-/-}$ mice. Neurons are only rarely infected in the CNS of wt mice following MHV-JHM v2.2-1 infection (14, 53). By contrast, extensive neuronal infection, especially within the hippocampus, was detected in IFNAR$^{-/-}$ mice (Fig. 3E and F). Neuronal infection was initially apparent as early as day 4 p.i. in IFNAR$^{-/-}$ mice and increased with time p.i. No demyelination was detected in the brains or spinal cords of either group at day 6 p.i. (data not shown).

Impaired IFN-I signaling increases neutrophil accumulation and proinflammatory signals. To reveal how reduced IFN-I in the CNS and increased viral replication affected recruitment of inflammatory cells, the magnitude and composition of CD45^{high} inflammatory cells were characterized by flow cytometry. Inflammation at 48 h p.i was limited but similar in the CNS of the two groups (less than 10% CD45^{high} cells). By day 4 p.i., leukocyte accumulation increased in infected IFNAR$^{-/-}$ compared to wt mice. This increase remained less than twofold throughout day 6 p.i. but increased dramatically by day 7 p.i. in the surviving IFNAR$^{-/-}$ mice (Fig. 4A). The minimal increase in bone marrow-derived inflammatory cells in the CNS of infected IFNAR $^{-/-}$ mice is consistent with similar

levels and distribution of inflammatory cells detected by immunohistochemistry (Fig. 3 and data not shown).

Analysis of the infiltrating cells revealed a prominent skewing towards Ly-6G$^+$ neutrophil accumulation in the CNS of IFNAR$^{-/-}$ mice (Fig. 4B). Neutrophils comprised the principal infiltrating population in the CNS of IFNAR$^{-/-}$ mice through day 5 p.i. By contrast, F4/80$^+$ macrophages prevailed in wt mice (Fig. 4B and C). Correspondingly, the proportion of macrophages in the CNS of IFNAR$^{-/-}$ mice was reduced compared to wt mice; however, they reached similar percentages by day 6 p.i. The proportion of NK cells was reduced in the CNS of IFNAR$^{-/-}$ mice (data not shown), consistent with findings in other models (32).

Neutrophils shape the inflammatory response within the CNS and are associated with severe clinical outcomes in other models of CNS inflammation (49, 54). Similarly, following MHV-JHM infection neutrophils play a role in regulating lymphocyte entry into the CNS (59). To assess whether the large neutrophil population played a role in disease severity, IFNAR$^{-/-}$ and wt mice were depleted of neutrophils via anti-Ly-6G/C (Gr-1) MAb treatment as previously described (59). Neutropenic IFNAR$^{-/-}$ mice showed no improvement in survival or clinical outcome following infection compared to isotype control-treated mice, indicating that neutrophils are not immunopathogenic (data not shown).

Expression of prominent proinflammatory mediators in response to CNS infection was further explored to correlate increased viral load with proinflammatory responses. Tumor necrosis factor alpha (TNF-α) was detected at day 5 p.i. in the CNS of IFNAR$^{-/-}$ mice (Fig. 5). No TNF-α was detected in the CNS of wt mice at day 5 p.i., although TNF-α mRNA is induced rapidly following MHV-JHM infection (35). By day 6 p.i. TNF-α was detected in the CNS of both groups, although levels were significantly higher in infected IFNAR $^{-/-}$ mice. While interleukin-6 (IL-6) and CCL2 (MCP-1) were detected at all time points p.i. in both groups (Fig. 5), levels were significantly increased in the CNS of IFNAR$^{-/-}$ mice. IL-10 and IL-12p70 remained undetectable in CNS supernatants in both groups throughout infection (data not shown). These data are consistent with exacerbation of proinflammatory responses to uncontrolled replication of MHV-JHM within the CNS.

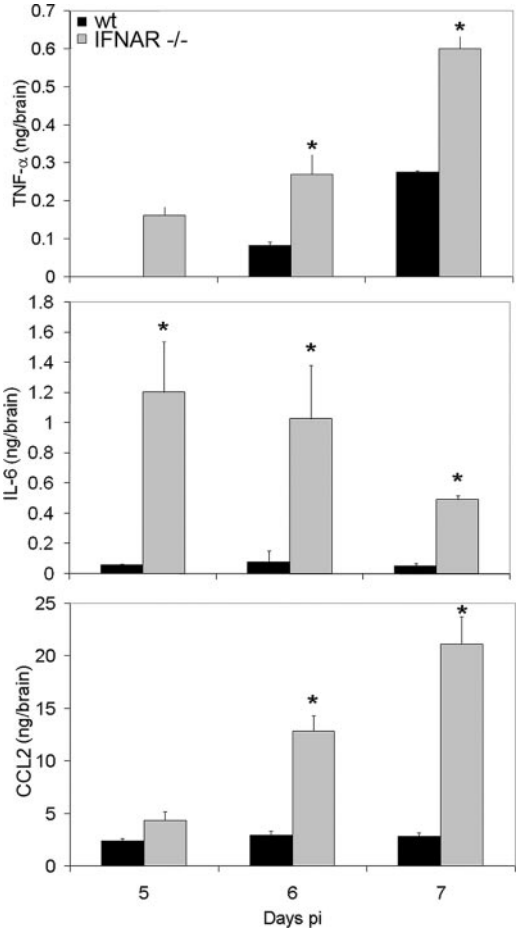

FIG. 5. Enhanced inflammatory responses in IFNAR$^{-/-}$ mice. CBA was used to measure the concentrations of inflammatory cytokines in brain supernatants of wt and IFNAR$^{-/-}$ mice. Bars indicate the mean concentrations of cytokines ± standard errors of the means. Data are derived from two independent experiments ($n = 6$ per time point). Asterisks indicate statistical significance ($P \leq 0.05$) in comparison to wt mice.

Impaired IFN-I signaling enhances bystander CD8 T-cell recruitment but does not impair expansion of virus-specific CD8 T cells. IFN-I can augment T-cell responses at multiple stages of infection (2, 47). Overall, the proportion of CD4 T cells in CNS infiltrates increased from days 5 to 7 p.i. in both groups of mice, although relative CD4 T-cell percentages within CNS infiltrates were consistently lower in infected IFNAR$^{-/-}$ mice (Fig. 4D). However, the proportions of CNS-infiltrating CD8 T cells were similar in infected IFNAR$^{-/-}$ and wt mice throughout infection, indicating that infiltration and accumulation of CD8 T cells in the CNS are IFN-I independent (Fig. 4E). CNS infection is associated with recruitment of a significant proportion of heterologous bystander CD8 T cells early during the response (9), which may negatively affect virus-specific CD8 T cells in the absence of IFN-I signaling (1). Inefficient virus-specific CD8 T-cell expansion or survival may thus contribute to uncontrolled virus replication in IFNAR$^{-/-}$ mice. The virus-specific population within total CNS CD8 T cells was indeed significantly lower in IFNAR$^{-/-}$ mice at day 6 p.i., when tetramer$^+$ cells began to accumulate in both groups of mice (Fig. 6). Furthermore, the proportion was still reduced compared to wt mice, despite the substantial increase of virus-specific T cells by day 7 p.i. However, taking overall greater CNS inflammation in IFNAR$^{-/-}$ mice into account, total numbers of virus-specific CD8 T cells were similar in the two groups, or even greater in the CNS of IFNAR$^{-/-}$ mice than in that of wt mice. Nevertheless, the reduced proportion of virus-specific CD8 T cells in the CNS suggested less-effective expansion or recruitment in the absence of IFN-I signaling. Emergence of tetramer$^+$ cells was thus analyzed in CLN, the primary site for priming of adaptive responses following CNS infections (27). Tetramer$^+$ cells were detected in the CLN as early as day 4 p.i., albeit numbers were very low (Fig. 6). By day 6 p.i., virus-specific CD8 T cells had expanded in both groups of mice; however, the frequency of tetramer$^+$ CD8 T cells increased fourfold in IFNAR$^{-/-}$ mice compared to wt mice. The virus-specific populations further expanded in both groups by day 7 p.i. without altering the relative ratio of tetramer$^+$ cells between the two groups. Deficiency in IFN-I responsive-

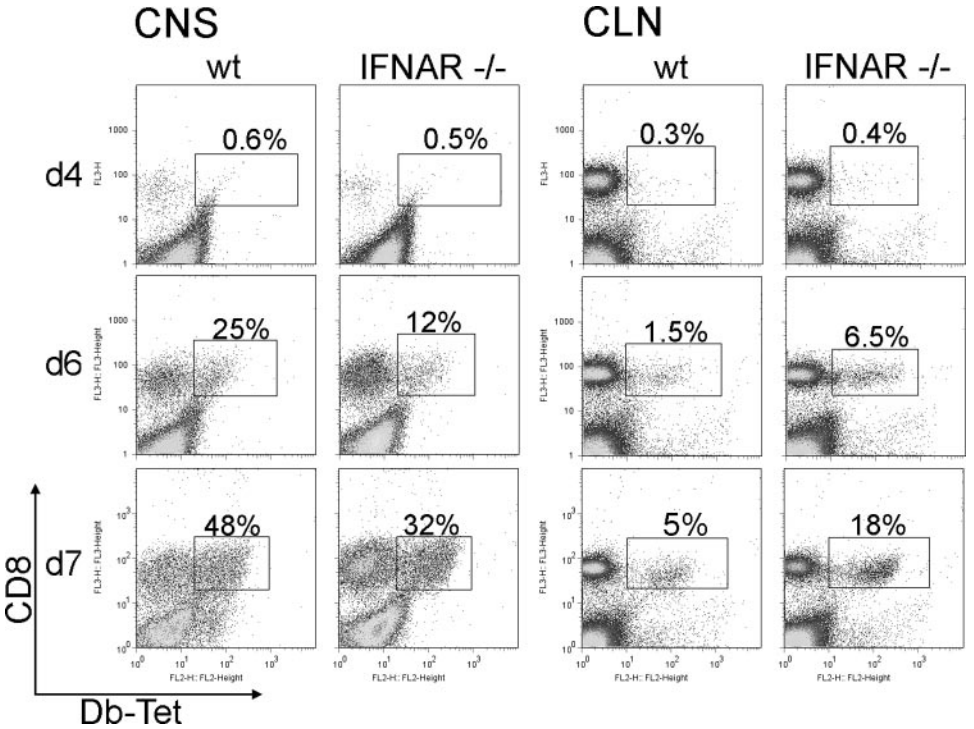

FIG. 6. Impaired IFN-I signaling does not affect expansion and CNS recruitment of virus-specific CD8 T cells. Cells derived from the CNS and CLN of infected mice were analyzed for the frequency of Db-S510-specific CD8 T cells by flow cytometry at the indicated days p.i. Representative density plots depict staining with anti-CD8 MAb and Db-S510 tetramer (Db-Tet) within the $CD45^{high}$ infiltrating cells and within CLN-derived cells, respectively. Boxed regions depict $tetramer^+$ CD8 T cells. Percentages represent the proportions of $tetramer^+$ cells within the CD8 T-cell population. Data shown are representative of three independent experiments.

ness thus did not impair priming or expansion of virus-specific CD8 T cells in the draining CLN. However, their decreased accumulation in the CNS suggested that virus-specific T cells generated in the CLN did not egress as efficiently in the absence of IFN-I, causing the majority of CD8 T cells in the CNS of $IFNAR^{-/-}$ mice to be bystander CD8 T cells (Fig. 6). $Tetramer^+$ cells in spleens of wt and $IFNAR^{-/-}$ mice were at similar levels (4% for wt and 3% for $IFNAR^{-/-}$ mice at day 7 p.i.), indicating that the observed effects on virus-specific CD8 T cells were specific to the CNS and draining CLN.

IFN-γ released by T cells constitutes the most critical effector mechanism required for control of sublethal MHV-JHM infection (4, 5). The in vivo functionality of T cells in the CNS was thus tested by measuring IFN-γ (Fig. 7). $IFNAR^{-/-}$ mice exhibited significantly higher levels of IFN-γ than did wt mice (Fig. 7A). Although elevated concentrations were already evident at day 5 p.i. in $IFNAR^{-/-}$ mice, they exceeded the levels in wt mice by greater than 10-fold at days 6 and 7 p.i. Enhanced IFN-γ secretion supports the notion that increased viral antigen leads to increased engagement of virus-specific CD8 T cells, which are also present at higher absolute numbers. T cells isolated from the CNS of infected mice were thus tested for their ability to produce IFN-γ. The frequency of IFN-γ-secreting cells was consistently elevated in $IFNAR^{-/-}$ relative to wt CNS-derived CD8 T cells at day 7 p.i. (Fig. 7B). Furthermore, whereas endogenous viral antigen in the culture elicited IFN-γ secretion in ~7% of wt CD8 T cells, ~50% of $IFNAR^{-/-}$ CD8 T cells produced IFN-γ in the absence of exogenous peptide. Exogenous peptide stimulation thus increased the frequency of IFN-γ-producing cells only modestly in $IFNAR^{-/-}$ CD8 T cells but by fivefold in wt CD8 T cells. The proportion of CNS CD4 T cells expressing IFN-γ was also notably higher in $IFNAR^{-/-}$ mice than in wt mice (Fig. 7C). Similarly to CD8 T cells, $IFNAR^{-/-}$-derived CD4 T cells were already stimulated to maximal levels by endogenous viral antigen (Fig. 7C). The high levels of stimulation of endogenous antigen are consistent with almost 100-fold-higher virus levels (Fig. 1) and vastly increased IFN-γ protein levels in the CNS of $IFNAR^{-/-}$ mice.

The scant evidence for viral clearance despite increased IFN-γ levels in the CNS of $IFNAR^{-/-}$ mice at 5 days p.i. suggested that viral load was already too high for effective perforin-mediated clearance. Alternatively, glia may not be responding to CD8 T-cell-mediated effector function. IFN-I signaling may be crucial to optimize antigen presentation in the early phases of CNS infection prior to IFN-γ-mediated signals. This is evident by early upregulation of class I on microglia, even in the absence of IFN-γ (5). The failure to control infection may therefore result from delayed MHC class I expression and antigen presentation by CNS-resident cells. Indeed, only a small percentage of microglia (10%) expressed class I at day 4 p.i. at barely detectable levels in the CNS of infected $IFNAR^{-/-}$ mice (Fig. 8A and B). Class I expression increased by day 6 p.i., coincident with high levels of IFN-γ. By contrast, ~40% of wt microglia expressed class I at day 4 p.i., and both the percentage and level of expression increased by day 6 p.i. Thus, class I expression on microglia was reduced in

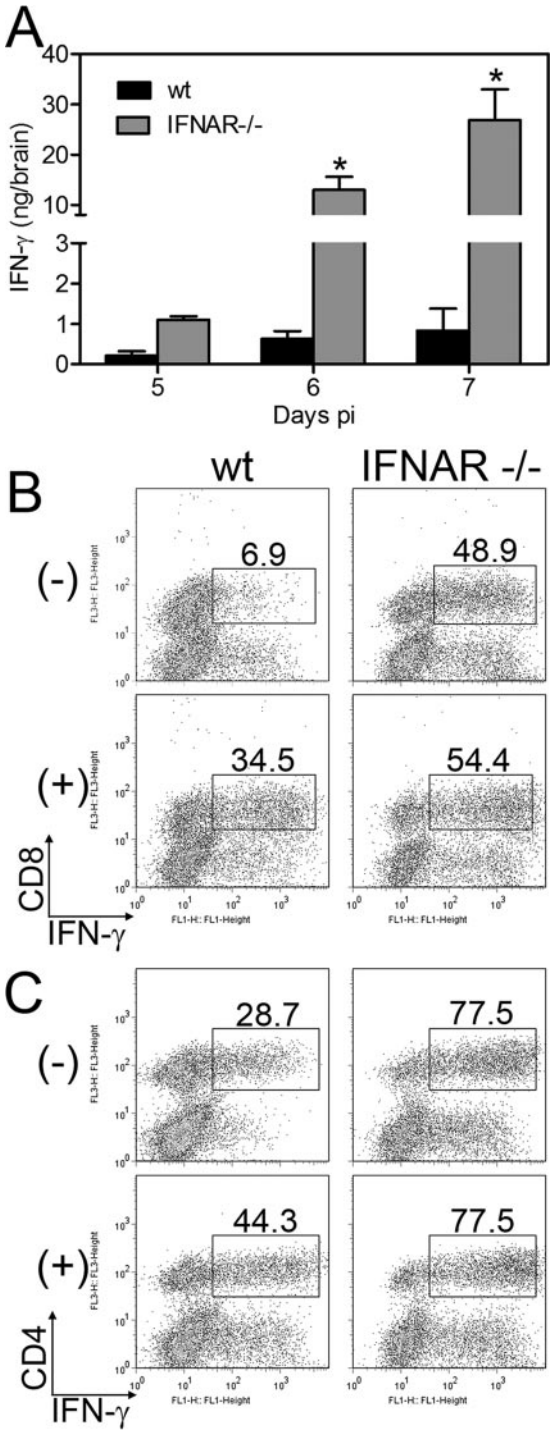

FIG. 7. IFN-I signaling does not regulate CD8 T-cell effector function. (A) IFN-γ levels measured by CBA in brain supernatants of infected mice. Data represent the mean IFN-γ concentrations from two combined experiments ± standard errors of the means ($n = 6$). Asterisks indicate statistical significance ($P \leq 0.05$) in comparison to wt mice. (B and C) Cells derived from brains at day 7 p.i. incubated in the absence (−) or presence (+) of S510 or M133 peptide for 6 h to stimulate virus-specific CD8 T cells (B) or CD4 T cells (C), respectively. EL-4 or CHB3 cells were used as CD8 or CD4 T-cell stimulator cells, respectively. Flow cytometry plots demonstrate intracellular staining for IFN-γ in CD8 T cells and CD4 T cells (gated on $CD45^{high}$ infiltrating cells). The numbers within each plot indicate the percentages of IFN-γ-positive cells within the T-cell population. Data are representative of two independent experiments.

infected $IFNAR^{-/-}$ mice with respect to frequency and expression levels. By contrast, nearly 100% of infiltrating, bone marrow-derived macrophages expressed class I at similar levels in the two groups (Fig. 8A and B). MHC class II upregulation on resident CNS cells is largely restricted to microglia and strictly IFN-γ dependent (19). It was thus expected that class II expression by microglia would be similar in $IFNAR^{-/-}$ mice. In fact, microglia and macrophages from the CNS of $IFNAR^{-/-}$ mice expressed frequencies and levels of class II expression similar to those of wt mice (Fig. 8C and D), confirming IFN-γ-driven class II expression.

DISCUSSION

The critical role of IFN-I in containing viral infections in vivo is demonstrated by the increased susceptibility of IFN-I-unresponsive mice to infections by a variety of RNA viruses (20, 31, 41). Infections in the absence of IFN-I invariably result in expanded tissue tropism, uncontrolled dissemination, and rapid mortality. Despite the inability of several MHV strains to induce IFN-I in fibroblasts and mature DC in vitro, they do induce these cytokines in pDC, neuronal cultures, and the CNS (8, 17, 39, 57). This study utilized nonlethal glia-tropic variants of MHV-JHM, which do not productively infect peripheral tissues, to dissect the pleiotropic effects of IFN-I in the context of a CNS infection controlled by CD8 T cells in wt mice. Infection of $IFNAR^{-/-}$ mice with both demyelinating and nondemyelinating variants resulted in uncontrolled replication and mortality. Similarly to uncontrolled replication of neurotropic MHV-JHM, an MHV-A59 mutant with a deletion in nonstructural protein 1 replicates uncontrolledly in peripheral tissues of $IFNAR^{-/-}$ animals but is highly attenuated in wt mice (61).

Although the number of glial cells infected was increased, IFN-I deficiency did not reveal preferential viral spread within a particular glial subset. Furthermore, tropism was expanded to neurons, which are rarely infected in wt mice (14). These results suggested that all glial cell types are responsive to IFN-I and that neurons are protected from infection by endogenous IFN-I-mediated pathways, a finding which has previously been implicated in the resistance of neurons from adult mice to Sindbis virus infection (6, 7).

The survival time following CNS MHV-JHM infection was prolonged relative to rapid death within 2 to 3 days following heterologous infection of $IFNAR^{-/-}$ mice with the dual liver- and CNS-tropic MHV-A59 variant (8). This allowed assessment of the effects of IFN-I deficiency on innate and adaptive immune responses. The most striking difference in the CNS inflammatory response was the domination of neutrophils in the CNS of $IFNAR^{-/-}$ mice, relative to predominant macrophages in wt mice. Macrophage recruitment appeared to be independent of IFN-I signaling, as indicated by similar overall numbers in the CNS of the two groups. Whether the skewing towards neutrophils reflects altered mononuclear cell populations in naïve $IFNAR^{-/-}$ mice (31), preferential accumulation of neutrophils due to increased virus replication and tissue destruction, or the absence of IFN-I-mediated regulation of the inflammatory response remains to be elucidated. Prominent neutrophil recruitment is associated with pathology and disease severity in the CNS autoimmune model experimental

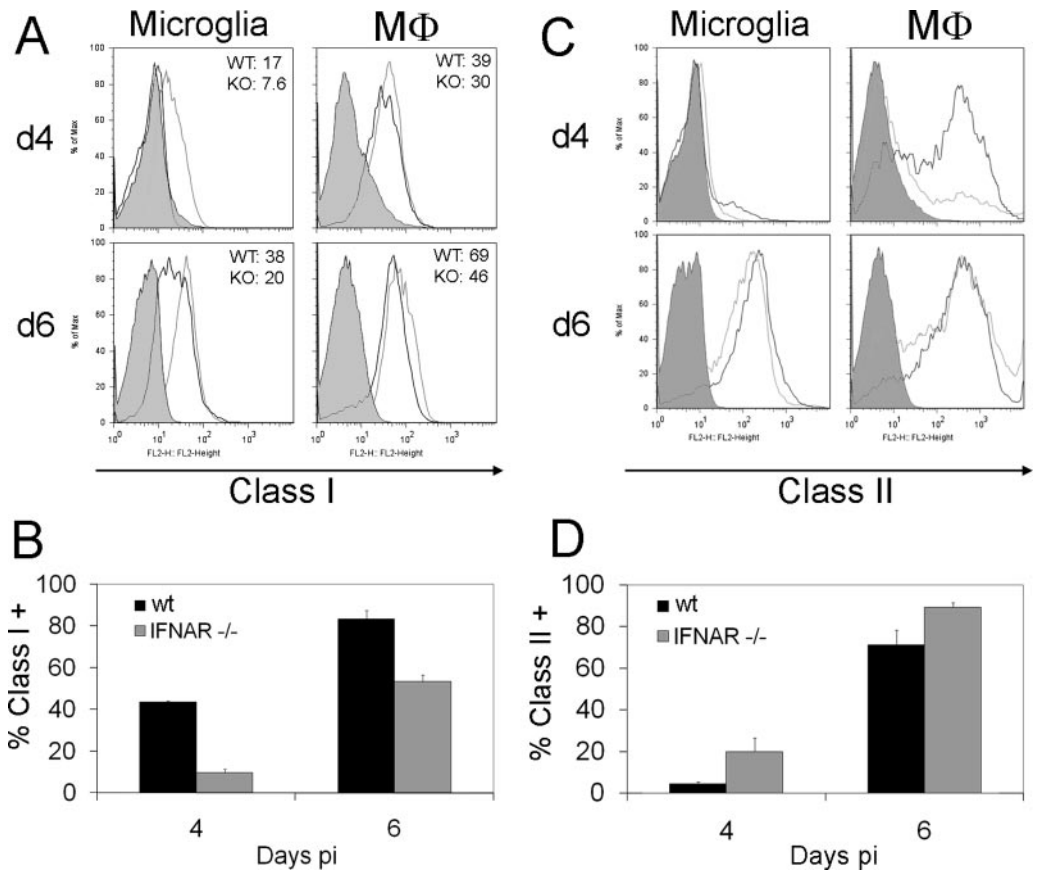

FIG. 8. MHC class I but not class II expression by microglia is reduced in the absence of IFN-I signaling. Cells isolated from the CNS were analyzed for MHC class I (H-2D^b) and class II (I-A^b) expression at the indicated times p.i. (A and C) Histograms revealing kinetics of class I (A) or class II (C) expression are gated on CD45^{low} microglia (left panels) and CD45^{high}, F4/80$^+$ bone marrow-derived infiltrating macrophages (right panels, MΦ). MHC class I or class II expression by wt cells is indicated by gray lines, and that by IFNAR$^{-/-}$ cells is indicated by black lines. Isotype control MAb staining is indicated by filled histograms. Numbers in the right corner of each plot in panel A indicate the mean fluorescence intensity of H-2D^b staining. Plots are representative of three independent experiments. (B and D) The proportion of microglia expressing class I (B) or class II (D) at the indicated days p.i. Data represent the means of three experiments ± standard errors of the means.

allergic encephalomyelitis (30, 33, 50, 54); however, depletion of neutrophils in IFNAR$^{-/-}$ mice did not affect virus replication or mortality rates. Increased neutrophil recruitment is also associated with a more virulent, lethal neurotropic strain of MHV-JHM in wt mice (59), suggesting that increased replication contributed partially to fatal disease outcome.

CD8 T cells play a crucial role in controlling acute MHV-JHM infection in the CNS via both perforin and IFN-γ (4, 5). IFN-I modulates CD8 T-cell immune responses through the induction of other cytokines, such as IL-15, or direct lymphocyte signaling (10). Nevertheless, different infections have shown distinct CD8 T-cell dependencies on IFN-I. LCMV infection is associated with a severe loss of virus-specific T cells in IFNAR$^{-/-}$ mice due to their dependence on IFN-I for survival (48). By contrast, infection of IFNAR$^{-/-}$ mice with vaccinia virus, vesicular stomatitis virus, or *Listeria monocytogenes* results only in a modest three- to fivefold decrease in T-cell expansion (48). Following Sendai virus infection, virus-specific CD8 T-cell survival and function are independent of IFN-I (25). Similar to the Sendai virus model, there was no evidence for impaired CD8 T-cell expansion in CLN or recruitment into the CNS during MHV-JHM infection. Preferential virus-specific CD8 T-cell accumulation only in CLN but not in spleen of infected IFNAR$^{-/-}$ mice ruled out enhanced virus-specific CD8 T-cell expansion due to dissemination to other lymphoid tissues. Upregulation of CD69 expression, which is prominently, but not exclusively, mediated by IFN-α/β, has been shown to limit egress of lymphocytes from lymphoid organs by downregulating $S1P_1$, a receptor required for lymphocyte egress (43). However, CD69 expression was not significantly altered in CLN-derived CD8 T cells from infected IFNAR$^{-/-}$ mice compared to wt mice (data not shown). Enhanced accumulation of virus-specific CD8 T cells may thus reflect increased viral antigen in CLN. No evident defects in CLN egress were supported by similar absolute numbers of virus-specific CD8 T cells in the CNS. Similarly to other infections, MHV-JHM results in early antigen-independent recruitment of bystander memory CD8 T cells (9). The enhanced frequencies of heterologous CD8 T cells in the CNS of IFNAR$^{-/-}$ mice were thus consistent with stronger overall inflammatory signals.

Significantly increased levels of TNF-α, IL-6, IFN-γ, and CCL2 correlated with uncontrolled viral replication. Thus, although IFN-I is known to enhance TNF-α and IL-6 expression,

induction of these cytokines was IFN-I independent. As NK cells do not contribute to viral clearance or IFN-γ-mediated MHC upregulation in the CNS (60), the high IFN-γ levels in the CNS of infected IFNAR$^{-/-}$ mice likely result from more-frequent T-cell engagement by the vastly increased numbers of infected cells. Indeed, this notion was supported by the increased frequencies of both CD4 and CD8 T cells expressing IFN-γ ex vivo in the absence of exogenous peptide stimulation. Nevertheless, the inability to control virus replication, despite increased IFN-γ levels even early during infection, suggests that T cells are unable to compensate for the overwhelming viral antigen load.

Reduced class I upregulation on microglia demonstrated that IFN-I plays a major role in enhancing antigen presentation early during infection and confirmed IFN-γ-independent class I expression on microglia (5). Nevertheless, persistently reduced levels of class I expression on resident glia in the CNS of infected IFNAR$^{-/-}$ mice, despite increased IFN-γ levels, were surprising. Reduced class I levels on microglia were not intrinsic to IFN-I signaling deficiency, as class I and class II molecule expression levels were similar on infiltrating macrophages. Furthermore, effective IFN-γ responsiveness was demonstrated by similar class II upregulation on microglia, known to be driven by IFN-γ-mediated CIITA activation (34). Thus, limited class I expression suggests cooperation between IFN-I and IFN-γ in driving optimal class I expression on this glial cell type. Cooperative regulation may also explain reduced transcription of OAS2, PKR, IFIT-1, and IFIT-2, despite high IFN-γ levels. Synergy is supported by common signaling pathways for IFN-I and IFN-γ (28) and has been demonstrated by enhanced antiviral effects of dual IFN-α and IFN-γ treatment during CoV infection (15).

The present results highlight the crucial role of IFN-I in directly limiting viral spread in CNS-resident glial cells. Furthermore, expanded tropism to neurons supports a protective role of constitutive IFN-I produced by neurons in limiting neuronal infection in wt mice. Importantly, the absence of impairment in virus-specific CD8 T-cell responses emphasized that regulation of CD8 T cells by IFN-I is clearly dependent on both the local milieu and the pathogen. Nevertheless, the inability of functional CD8 T cells to control virus suggests that an initial set point of infected cells, relative to infiltrating virus-specific T cells, determines the outcome of a protective T-cell response. During MHV-JHM CNS infection this threshold is clearly controlled by direct antiviral IFN-I function.

ACKNOWLEDGMENTS

This work was supported by National Institutes of Health grants NS18146 and AI47249.

We thank Wen Wei, Ernesto Baron, and Anthony Rodriguez for excellent assistance with the histopathology.

REFERENCES

1. **Bahl, K., S. K. Kim, C. Calcagno, D. Ghersi, R. Puzone, F. Celada, L. K. Selin, and R. M. Welsh.** 2006. IFN-induced attrition of CD8 T cells in the presence or absence of cognate antigen during the early stages of viral infections. J. Immunol. **176:**4284–4295.
2. **Bailey, S. L., P. A. Carpentier, E. J. McMahon, W. S. Begolka, and S. D. Miller.** 2006. Innate and adaptive immune responses of the central nervous system. Crit. Rev. Immunol. **26:**149–188.
3. **Bergmann, C. C., J. D. Altman, D. Hinton, and S. A. Stohlman.** 1999. Inverted immunodominance and impaired cytolytic function of CD8+ T cells during viral persistence in the central nervous system. J. Immunol. **163:**3379–3387.
4. **Bergmann, C. C., T. E. Lane, and S. A. Stohlman.** 2006. Coronavirus infection of the central nervous system: host-virus stand-off. Nat. Rev. Microbiol. **4:**121–132.
5. **Bergmann, C. C., B. Parra, D. R. Hinton, R. Chandran, M. Morrison, and S. A. Stohlman.** 2003. Perforin-mediated effector function within the central nervous system requires IFN-gamma-mediated MHC up-regulation. J. Immunol. **170:**3204–3213.
6. **Burdeinick-Kerr, R., J. Wind, and D. E. Griffin.** 2007. Synergistic roles of antibody and interferon in noncytolytic clearance of Sindbis virus from different regions of the central nervous system. J. Virol. **81:**5628–5636.
7. **Byrnes, A. P., J. E. Durbin, and D. E. Griffin.** 2000. Control of Sindbis virus infection by antibody in interferon-deficient mice. J. Virol. **74:**3905–3908.
8. **Cervantes-Barragan, L., R. Zust, F. Weber, M. Spiegel, K. S. Lang, S. Akira, V. Thiel, and B. Ludewig.** 2007. Control of coronavirus infection through plasmacytoid dendritic cell-derived type I interferon. Blood **109:**1131–1137.
9. **Chen, A. M., N. Khanna, S. A. Stohlman, and C. C. Bergmann.** 2005. Virus-specific and bystander CD8 T cells recruited during virus-induced encephalomyelitis. J. Virol. **79:**4700–4708.
10. **Curtsinger, J. M., J. O. Valenzuela, P. Agarwal, D. Lins, and M. F. Mescher.** 2005. Type I IFNs provide a third signal to CD8 T cells to stimulate clonal expansion and differentiation. J. Immunol. **174:**4465–4469.
11. **Dafny, N., and P. B. Yang.** 2005. Interferon and the central nervous system. Eur. J. Pharmacol. **523:**1–15.
12. **Delhaye, S., S. Paul, G. Blakqori, M. Minet, F. Weber, P. Staeheli, and T. Michiels.** 2006. Neurons produce type I interferon during viral encephalitis. Proc. Natl. Acad. Sci. USA **103:**7835–7840.
13. **Fleming, J. O., M. D. Trousdale, F. A. el-Zaatari, S. A. Stohlman, and L. P. Weiner.** 1986. Pathogenicity of antigenic variants of murine coronavirus JHM selected with monoclonal antibodies. J. Virol. **58:**869–875.
14. **Fleming, J. O., M. D. Trousdale, S. A. Stohlman, and L. P. Weiner.** 1987. Pathogenic characteristics of neutralization-resistant variants of JHM coronavirus (MHV-4). Adv. Exp. Med. Biol. **218:**333–342.
15. **Fuchizaki, U., S. Kaneko, Y. Nakamoto, Y. Sugiyama, K. Imagawa, M. Kikuchi, and K. Kobayashi.** 2003. Synergistic antiviral effect of a combination of mouse interferon-alpha and interferon-gamma on mouse hepatitis virus. J. Med. Virol. **69:**188–194.
16. **Galea, I., I. Bechmann, and V. H. Perry.** 2007. What is immune privilege (not)? Trends Immunol. **28:**12–18.
17. **Garlinghouse, L. E. J., A. L. Smith, and T. Holford.** 1984. The biological relationship of mouse hepatitis virus (MHV) strains and interferon: in vitro induction and sensitivities. Arch. Virol. **82:**19–29.
18. **Haring, J. S., L. L. Pewe, and S. Perlman.** 2001. High-magnitude, virus-specific CD4 T-cell response in the central nervous system of coronavirus-infected mice. J. Virol. **75:**3043–3047.
19. **Horwitz, M. S., C. F. Evans, F. G. Klier, and M. B. Oldstone.** 1999. Detailed in vivo analysis of interferon-gamma induced major histocompatibility complex expression in the central nervous system: astrocytes fail to express major histocompatibility complex class I and II molecules. Lab. Investig. **79:**235–242.
20. **Ida-Hosonuma, M., T. Iwasaki, T. Yoshikawa, N. Nagata, Y. Sato, T. Sata, M. Yoneyama, T. Fujita, C. Taya, H. Yonekawa, and S. Koike.** 2005. The alpha/beta interferon response controls tissue tropism and pathogenicity of poliovirus. J. Virol. **79:**4460–4469.
21. **Kawai, T., and S. Akira.** 2006. Innate immune recognition of viral infection. Nat. Immunol. **7:**131–137.
22. **Kolumam, G. A., S. Thomas, L. J. Thompson, J. Sprent, and K. Murali-Krishna.** 2005. Type I interferons act directly on CD8 T cells to allow clonal expansion and memory formation in response to viral infection. J. Exp. Med. **202:**637–650.
23. **Kopecky-Bromberg, S. A., L. Martinez-Sobrido, M. Frieman, R. A. Baric, and P. Palese.** 2007. Severe acute respiratory syndrome coronavirus open reading frame (ORF) 3b, ORF 6, and nucleocapsid proteins function as interferon antagonists. J. Virol. **81:**548–557.
24. **Lavi, E., and Q. Wang.** 1995. The protective role of cytotoxic T cells and interferon against coronavirus invasion of the brain. Adv. Exp. Med. Biol. **380:**145–149.
25. **Lopez, C. B., J. S. Yount, T. Hermesh, and T. M. Moran.** 2006. Sendai virus infection induces efficient adaptive immunity independently of type I interferons. J. Virol. **80:**4538–4545.
26. **Marten, N. W., S. A. Stohlman, R. D. Atkinson, D. R. Hinton, J. O. Fleming, and C. C. Bergmann.** 2000. Contributions of CD8+ T cells and viral spread to demyelinating disease. J. Immunol. **164:**4080–4088.
27. **Marten, N. W., S. A. Stohlman, J. Zhou, and C. C. Bergmann.** 2003. Kinetics of virus-specific CD8$^+$-T-cell expansion and trafficking following central nervous system infection. J. Virol. **77:**2775–2778.
28. **Matsumoto, M., N. Tanaka, H. Harada, T. Kimura, T. Yokochi, M. Kitagawa, C. Schindler, and T. Taniguchi.** 1999. Activation of the transcription factor ISGF3 by interferon-gamma. Biol. Chem. **380:**699–703.
29. **Matsuyama, S., S. Henmi, N. Ichihara, S. Sone, T. Kikuchi, T. Ariga, and F. Taguchi.** 2000. Protective effects of murine recombinant interferon-beta administered by intravenous, intramuscular or subcutaneous route on mouse hepatitis virus infection. Antivir. Res. **47:**131–137.

30. **McColl, S. R., M. A. Staykova, A. Wozniak, S. Fordham, J. Bruce, and D. O. Willenborg.** 1998. Treatment with anti-granulocyte antibodies inhibits the effector phase of experimental autoimmune encephalomyelitis. J. Immunol. **161:**6421–6426.
31. **Muller, U., U. Steinhoff, L. F. Reis, S. Hemmi, J. Pavlovic, R. M. Zinkernagel, and M. Aguet.** 1994. Functional role of type I and type II interferons in antiviral defense. Science **264:**1918–1921.
32. **Nguyen, K. B., T. P. Salazar-Mather, M. Y. Dalod, J. B. Van Deusen, X. Q. Wei, F. Y. Liew, M. A. Caligiuri, J. E. Durbin, and C. A. Biron.** 2002. Coordinated and distinct roles for IFN-alpha beta, IL-12, and IL-15 regulation of NK cell responses to viral infection. J. Immunol. **169:**4279–4287.
33. **Nygardas, P. T., J. A. Maatta, and A. E. Hinkkanen.** 2000. Chemokine expression by central nervous system resident cells and infiltrating neutrophils during experimental autoimmune encephalomyelitis in the BALB/c mouse. Eur. J. Immunol. **30:**1911–1918.
34. **O'Keefe, G. M., V. T. Nguyen, L. L. Ping Tang, and E. N. Benveniste.** 2001. IFN-gamma regulation of class II transactivator promoter IV in macrophages and microglia: involvement of the suppressors of cytokine signaling-1 protein. J. Immunol. **166:**2260–2269.
35. **Parra, B., D. R. Hinton, M. T. Lin, D. J. Cua, and S. A. Stohlman.** 1997. Kinetics of cytokine mRNA expression in the central nervous system following lethal and nonlethal coronavirus-induced acute encephalomyelitis. Virology **233:**260–270.
36. **Prehaud, C., F. Megret, M. Lafage, and M. Lafon.** 2005. Virus infection switches TLR-3-positive human neurons to become strong producers of beta interferon. J. Virol. **79:**12893–12904.
37. **Rempel, J. D., S. J. Murray, J. Meisner, and M. J. Buchmeier.** 2004. Differential regulation of innate and adaptive immune responses in viral encephalitis. Virology **318:**381–392.
38. **Rempel, J. D., L. A. Quina, P. K. Blakely-Gonzales, M. J. Buchmeier, and D. L. Gruol.** 2005. Viral induction of central nervous system innate immune responses. J. Virol. **79:**4369–4381.
39. **Roth-Cross, J. K., L. Martinez-Sobrido, E. P. Scott, A. Garcia-Sastre, and S. R. Weiss.** 2007. Inhibition of the alpha/beta interferon response by mouse hepatitis virus at multiple levels. J. Virol. **81:**7189–7199.
40. **Ryman, K. D., W. B. Klimstra, K. B. Nguyen, C. A. Biron, and R. E. Johnston.** 2000. Alpha/beta interferon protects adult mice from fatal Sindbis virus infection and is an important determinant of cell and tissue tropism. J. Virol. **74:**3366–3378.
41. **Samuel, M. A., and M. S. Diamond.** 2005. Alpha/beta interferon protects against lethal West Nile virus infection by restricting cellular tropism and enhancing neuronal survival. J. Virol. **79:**13350–13361.
42. **Serafini, B., S. Columba-Cabezas, F. Di Rosa, and F. Aloisi.** 2000. Intracerebral recruitment and maturation of dendritic cells in the onset and progression of experimental autoimmune encephalomyelitis. Am. J. Pathol. **157:**1991–2002.
43. **Shiow, L. R., D. B. Rosen, N. Brdickova, Y. Xu, J. An, L. L. Lanier, J. G. Cyster, and M. Matloubian.** 2006. CD69 acts downstream of interferon-alpha/beta to inhibit S1P1 and lymphocyte egress from lymphoid organs. Nature **440:**540–544.
44. **Smith, A. L., S. W. Barthold, and D. S. Beck.** 1987. Intranasally administered alpha/beta interferon prevents extension of mouse hepatitis virus, strain JHM, into the brains of BALB/cByJ mice. Antivir. Res. **8:**239–245.
45. **Spiegel, M., A. Pichlmair, L. Martinez-Sobrido, J. Cros, A. Garcia-Sastre, O. Haller, and F. Weber.** 2005. Inhibition of beta interferon induction by severe acute respiratory syndrome coronavirus suggests a two-step model for activation of interferon regulatory factor 3. J. Virol. **79:**2079–2086.
46. **Stetson, D. B., and R. Medzhitov.** 2006. Type I interferons in host defense. Immunity **25:**373–381.
47. **Theofilopoulos, A. N., R. Baccala, B. Beutler, and D. H. Kono.** 2005. Type I interferons (alpha/beta) in immunity and autoimmunity. Annu. Rev. Immunol. **23:**307–336.
48. **Thompson, L. J., G. A. Kolumam, S. Thomas, and K. Murali-Krishna.** 2006. Innate inflammatory signals induced by various pathogens differentially dictate the IFN-I dependence of CD8 T cells for clonal expansion and memory formation. J. Immunol. **177:**1746–1754.
49. **Tran, E. H., E. N. Prince, and T. Owens.** 2000. IFN-gamma shapes immune invasion of the central nervous system via regulation of chemokines. J. Immunol. **164:**2759–2768.
50. **Veldhuis, W. B., S. Floris, P. H. van der Meide, I. M. Vos, H. E. de Vries, C. D. Dijkstra, P. R. Bar, and K. Nicolay.** 2003. Interferon-beta prevents cytokine-induced neutrophil infiltration and attenuates blood-brain barrier disruption. J. Cereb. Blood Flow Metab. **23:**1060–1069.
51. **Versteeg, G. A., P. J. Bredenbeek, S. H. van den Worm, and W. J. Spaan.** 2007. Group 2 coronaviruses prevent immediate early interferon induction by protection of viral RNA from host cell recognition. Virology **361:**18–26.
52. **Versteeg, G. A., O. Slobodskaya, and W. J. Spaan.** 2006. Transcriptional profiling of acute cytopathic murine hepatitis virus infection in fibroblast-like cells. J. Gen. Virol. **87:**1961–1975.
53. **Wang, F. I., D. R. Hinton, W. Gilmore, M. D. Trousdale, and J. O. Fleming.** 1992. Sequential infection of glial cells by the murine hepatitis virus JHM strain (MHV-4) leads to a characteristic distribution of demyelination. Lab. Investig. **66:**744–754.
54. **Willenborg, D. O., S. Fordham, C. C. Bernard, W. B. Cowden, and I. A. Ramshaw.** 1996. IFN-gamma plays a critical down-regulatory role in the induction and effector phase of myelin oligodendrocyte glycoprotein-induced autoimmune encephalomyelitis. J. Immunol. **157:**3223–3227.
55. **Ye, Y., K. Hauns, J. O. Langland, B. L. Jacobs, and B. G. Hogue.** 2007. Mouse hepatitis coronavirus A59 nucleocapsid protein is a type I interferon antagonist. J. Virol. **81:**2554–2563.
56. **Zhou, H., and S. Perlman.** 2007. Mouse hepatitis virus does not induce beta interferon synthesis and does not inhibit its induction by double-stranded RNA. J. Virol. **81:**568–574.
57. **Zhou, H., and S. Perlman.** 2006. Preferential infection of mature dendritic cells by mouse hepatitis virus strain JHM. J. Virol. **80:**2506–2514.
58. **Zhou, J., N. W. Marten, C. C. Bergmann, W. B. Macklin, D. R. Hinton, and S. A. Stohlman.** 2005. Expression of matrix metalloproteinases and their tissue inhibitor during viral encephalitis. J. Virol. **79:**4764–4773.
59. **Zhou, J., S. A. Stohlman, D. R. Hinton, and N. W. Marten.** 2003. Neutrophils promote mononuclear cell infiltration during viral-induced encephalitis. J. Immunol. **170:**3331–3336.
60. **Zuo, J., S. A. Stohlman, J. B. Hoskin, D. R. Hinton, R. Atkinson, and C. C. Bergmann.** 2006. Mouse hepatitis virus pathogenesis in the central nervous system is independent of IL-15 and natural killer cells. Virology **350:**206–215.
61. **Zust, R., L. Cervantes-Barragan, T. Kuri, G. Blakqori, F. Weber, B. Ludewig, and V. Thiel.** 2007. Coronavirus nonstructural protein 1 is a major pathogenicity factor: implications for the rational design of coronavirus vaccines. PLoS Pathog. **3:**e109.